

# Diagnosis of Liver Disease Using Gaussian Blur Algorithm

<sup>1</sup> Devishree.V, <sup>2</sup> Bhavya S.N, <sup>3</sup> AnjaliNair.A, <sup>4</sup>M Thanuja  
<sup>1,2,3</sup>Student, <sup>4</sup>Asst.Proffessor

Department of ECE, AMC Engineering College, Bangalore, India

**Abstract** - In this paper, the classification of liver diseases using first-order statistics (FOS) is implemented for automatic preliminary diagnosis of liver diseases. Region of interest (ROI) extracted from MRI images are used as the input to characterize different tissue, namely liver cyst, fatty liver and healthy liver using first-order statistics. The results for first-order statistics are given. The measurements extracted from First-order statistic include entropy and correlation achieved obvious classification range in detecting different tissues in this work.

**Keywords** - Classification, first-order statistics, Magnetic Resonance Imaging (MRI), region of interest, Gaussian Blur, Morphological Application

## I. INTRODUCTION

LIVER cyst and fatty liver has become common health problems in United States and other Western countries due to the increase number of liver disease patients. Among the various image modalities available for liver disease diagnosis, MRI imaging techniques are currently the most popular [1]. A magnetic field is used to make the body's cells vibrate. The vibrations give off electrical signals which are interpreted by a computer and turned into very detailed images of "slices" of the body. MRI may be used to make images of every part of the body, including the bones, joints, blood vessels, nerves, muscles and organs. Different types of tissue show up in different colours, or more commonly grey-scale intensities on a computer-generated image. One advantage of MRI is that it produces one of the clearest images as compared to other non-ionizing imaging techniques such as Ultrasound [2]. Besides that, MRI images are also known to give more information and better contrast as compared to other modalities [3].

### Healthy Liver

Fig. 1 below depicts a healthy liver in an MRI image. The border of the liver regions are highlighted. In order to better understand the differences of the diseases and the image modalities used in this research, some of the 142 test images are described in this research work. The 142 test images used in this study were pre-diagnosed by a senior specialist at collaborating hospital, Hospital Selayang, Malaysia.

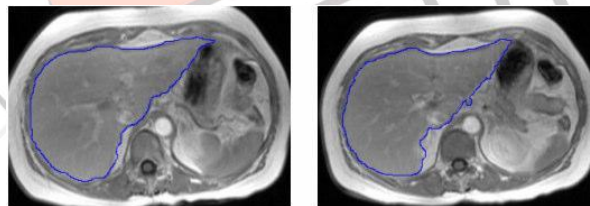
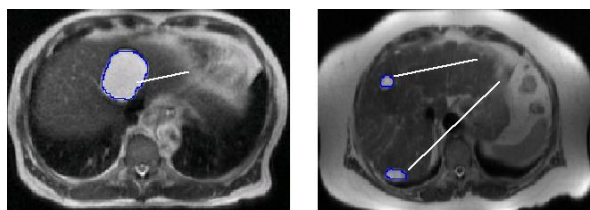


Fig. 1. Healthy liver MRI test image with the boundary of the liver region highlighted.

### Liver Cysts

Examples of cysts present in MRI are given in Fig. 2, with the border of the liver cyst region highlighted. The contour of the liver cyst is smooth, and the contrast between normal liver tissue and the liver cyst is high [2]. Fig. 2 (a) shows a clearly visible cyst in an abnormal liver while Fig. 2 (b) depicts almost invisible cysts in an abnormal liver in an MRI abdomen image.



(a) single cyst (b) multiple small cysts

Fig. 2. Identified liver cyst(s) structure in MRI images.

### Fatty Liver

Fig. 3 below depicts examples of fatty liver in the MRI modality. The boundary of the fatty liver regions are highlighted

**II. FIRST ORDER STATISTICS**

The first-order statistics (FOS) [7] can be derived from the grey-level histogram {  $h_i$  }, where  $h_i$  is the number of pixels with grey-level  $i$  in an image. Let  $N$  be the total number of pixels and  $G$  be the number of grey-levels,

hence  $\sum(h_i=N)$ . The normalized histogram {  $H_i$  } with  $h_i / N$

empirical probability density function for single pixels. Statistical methods analyze the spatial distribution of grey values using FOS by computing local features at each point in the image .

Derivation of a set of statistics from the distributions of the local features has been done by successfully in recent research works [9]. The use of statistical features is one of the early methods proposed in the literature [10] and can be classified into first-order (one pixel), second-order (two pixels) and higher-order (three or more pixels) statistics based on the number of pixels defining the local feature [11]. The FOS estimates properties of individual pixel values, ignoring the spatial interaction between pixels while second- and higher-order statistics on the other hand estimate the properties of two or more pixel values occurring at specific locations relative to each other [12]. Seven features are listed as given by equation below:

**Average Grey Level,  $\mu = \sum i H_i$**

**Standard Deviation,  $\sigma = (\sum (i-\mu)^2 H_i)^{1/2}$**

where  $\sigma$  measures the global contrast in the image and  $\mu$  is the average pixel intensity.

**Entropy,  $s = - \sum_{i=0}^{G-1} H_i \log H_i$**

where  $s$  measures the uniformity of the histogram [13]. This quantity is widely used in image compression.

**Correlation,  $C(P_{i,j}) = \frac{\sum_{i=0}^{L-1} \sum_{j=0}^{L-1} (i - \alpha_x)(j - \alpha_y) P_{d,\theta}(i,j)}{\alpha_x \alpha_y}$**

Correlation measures the linearity of a texture and the degree to which rows and columns resemble each other. Linearity is defined as the linear dependency of grey-levels of neighboring pixels.

**III. FOS IMPLEMENTATION**

In constructing the sparse coding for FOS, an image block of the ROI is drawn on the suspected area of liver diseases. For each acquired image, an ROI image of block 5 x 5 pixels is selected to produce FOS matrices as shown in Fig.5 for suspected areas of cysts

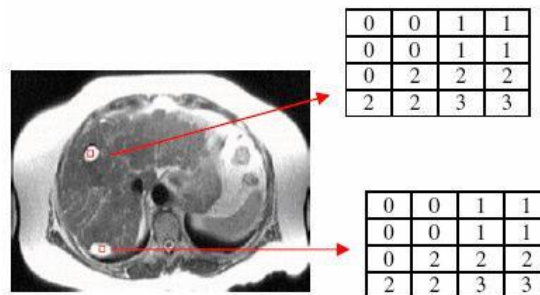
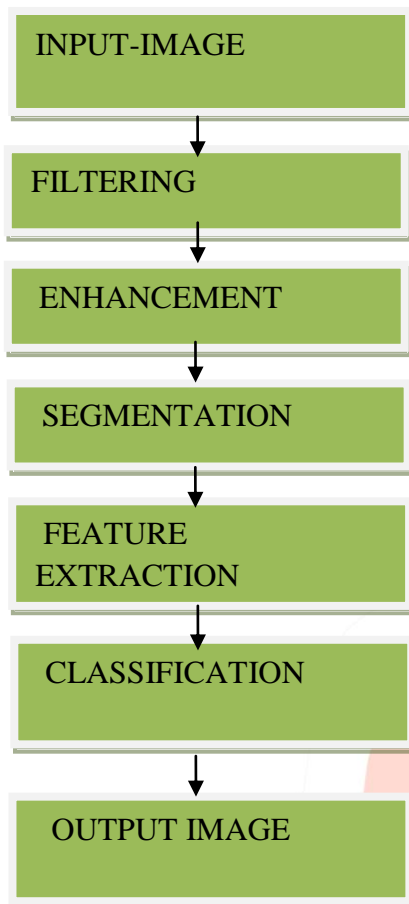


Fig. 5. Image block with the size of 5 x 5 pixels drawn on suspected liver cyst in liver MRI image.

The block is chosen, if possible, to include solely liver parenchyma, without major blood vessel at biliary ducts that can significantly affect the texture obtained

**FLOW CHART**



## I. FILTERING

Filtering in image processing allows for selective high lighting of specific information. Number of techniques available such as

1. Median Filter
2. Gaussian Filter

**A. Gaussian noise** - In telecommunications and computer networking, communication channels can be affected by wideband Gaussian noise coming from many natural sources, such as the thermal vibrations of atoms in conductors (referred to as thermal noise or Johnson-Nyquist noise) and other warm objects, and from celestial demonstrate the image with Gaussian noise.

**B. Salt and Pepper noise** - Salt and Pepper noise is a type of noise typically seen on images [3]. It is black and white pixels on an image at any random position. "Fig. 2" demonstration of Pepper noise.

## II. SPATIAL DOMAIN DIGITAL IMAGE FILTERS

The term spatial refers to image plane itself. Spatial domain image processing methods directly process the pixel. Spatial domain methods can be denoted as  $b(x, y) = F[a(x, y)]$ . Where  $a(x, y)$  is input image and  $b(x, y)$  is output image and  $F$  is some process over input image, defined over some neighbourhood pixels  $(x, y)$ .  $F$  can perform on set of input images, such as pixel by pixel sum of  $K$  images [1].

There are two types of image filters in spatial domain. 1) Smoothing spatial filters and 2) Sharpening spatial filters. There both can be linear or non-linear. Linear filter replaces each pixel by weighted sum of its neighbours. The matrix defining of neighbourhood pixels also specifies the weight assigned to each neighbour. This matrix is called kernel. The output of non-linear function is not linear function of inputs. Non-linear filter is based on conditioning on the neighbourhood pixels. For example output pixel is the mean of its neighbours is linear and select maximum pixel value from its neighbour is non-linear filter. A. Smoothing spatial filters

Smoothing spatial filters used for blurring and for noise reduction [1]. The objective of such filter is to reduce the amplitude of image variations [6]. It removes small details from image for example it removes small gaps in lines or curves [1].

Some linear smoothing filters in spatial domain are:

### 1) Mean Filter

This filter computes the output pixel by calculating the statistical mean of neighbourhood pixels of input pixel.

Mean filter replace each pixel in input image  $f$  with the average intensity in a  $3 \times 3$  (or  $5 \times 5$  or any other kernel) neighbourhood of pixels centred there. Then if  $g$  is the filtered image, it is defined by eq. 1.

$$g(i, j) = (f(i-1, j-1) + f(i-1, j) + f(i-1, j+1) + f(i, j-1) + f(i, j) + f(i, j+1) + f(i+1, j-1) + f(i+1, j) + f(i+1, j+1))/9$$

Where, (i, j) is pixel at ith row and jth column. We can think of this filtering operation in terms of the mask.

**2) Gaussian Filter**

A Gaussian blur (also known as Gaussian smoothing) is the result of blurring an image by a Gaussian function. It is a widely used effect in graphics software, typically to reduce image noise and reduce detail. The visual effect of this blurring technique is a smooth blur resembling that of viewing the image through a translucent screen. Gaussian smoothing is also used as a pre-processing stage in computer vision algorithms in order to enhance image

The following structures are,

Fig.1 Image with Gaussian Noise.

Fig.2. Image with Salt and Pepper Noise.

Fig.3 Demonstrate the Mean Filter.

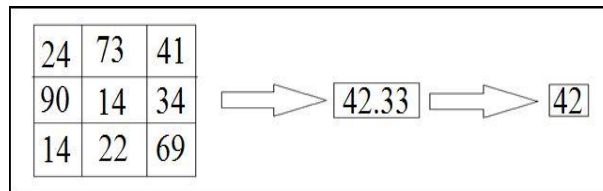


Fig.1 Image with Gaussian Noise

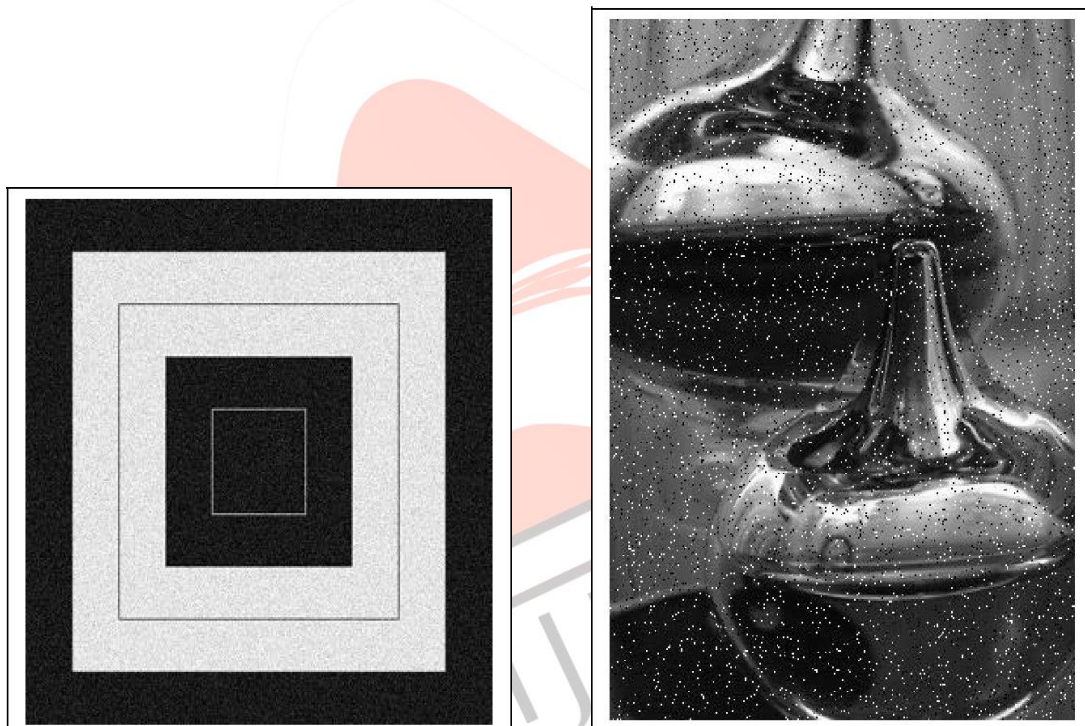


Fig2. Image with Salt and Pepper Noise

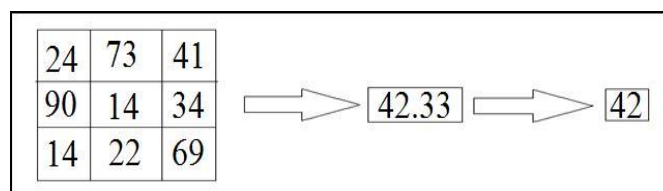


Fig.3 Demonstrate the Mean Filter

**II. ENHANCEMENT**

Enhancement refers accentuation, or sharpening of image features such as boundaries or contrast.

The enhancement methods can broadly be divided in to the following two categories:

1. Spatial Domain Methods
2. Frequency Domain Methods

**Spatial Domain Method**

In spatial domain techniques , we directly deal with the image pixels. The pixel values are manipulated to achieve desired enhancement.

### Frequency Domain Method

In frequency domain methods, the image is first transferred into the frequency domain. It means that, the Fourier Transform of the image is computed first. All the enhancement operations are performed on the Fourier transform of the image and then the Inverse Fourier transform is performed to get the resultant image. These enhancement operations are performed in order to modify the image brightness, contrast or the distribution of the grey levels.

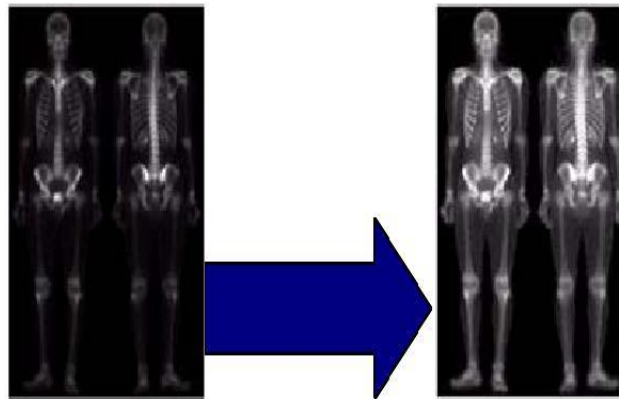
Image enhancement simply means, transforming an image  $f$  into image  $g$  using  $T$ . (Where  $T$  is the transformation. The values of pixels in images  $f$  and  $g$  are denoted by  $r$  and  $s$ , respectively. As said, the pixel values  $r$  and  $s$  are related by the expression,

$$s = T(r) \quad (1)$$

Where  $T$  is a transformation that maps a pixel value  $r$  into a pixel value  $s$ . The results of this transformation are mapped into the grey scale range as we are dealing here only with grey scale digital images. So, the results are mapped back into the range  $[0, L-1]$ , where  $L=2^k$ ,  $k$  being the number of bits in the image being considered. So, for instance, for an 8-bit image the range of pixel values will be  $[0, 255]$ .

I will consider only gray level images. The same theory can be extended for the color images too. A digital gray image can have pixel values in the range of 0 to 255.

**Fig. shows the effect to image enhancement.**



### III.SEGMENTATION

Segmentation is a process of partitioning a digital image into multiple segments. It is used to locate objects and boundaries in the image.

A. Segmentation Based on Edge Detection This method attempts to resolve image segmentation by detecting the edges or pixels between different regions that have rapid transition in intensity are extracted [1, 5] and linked to form closed object boundaries. The result is a binary image. Based on theory there are two main edge based segmentation methods- gray histogram and gradient based method.

#### 1. Gray Histogram Technique

The result of edge detection technique depends mainly on selection of threshold  $T$ , and it is really difficult to search for maximum and minimum gray level intensity because gray histogram is uneven for the impact of noise, thus we approximately substitute the curves of object and background with two conic Gaussian curves, whose intersection is the valley of histogram. Threshold  $T$  is the gray value of intersection point of that valley.

#### 2. Gradient Based Method

Gradient is the first derivative for image  $f(x, y)$ , when there is abrupt change in intensity near edge and there is little image noise, gradient based method works well. This method involves convolving gradient operators with the image. High value of the gradient magnitude is possible place of rapid transition between two different regions. These are edge pixels, they have to be linked to form closed boundaries of the regions. Common edge detection operators used in gradient based method are sobel operator, canny operator, Laplace operator, Laplacian of Gaussian (LOG) operator & so on, canny is most promising one, but takes more time as compared to sobel operator. Edge detection methods require a balance between detecting accuracy and noise immunity in practice, if the level of detecting accuracy is too high, noise may bring in fake edges making the outline of images unreasonable and if the degree of noise immunity is too excessive, some parts of the image outline may get undetected and the position of objects may be mistaken. Thus, edge detection algorithms are suitable for images that are simple and noise-free as well often produce missing edges or extra edges on complex and noisy images.

1. Snakes Active contours or snakes are computer generated curves [15-16] that move within the image to find object boundaries under the influence of internal and external forces. This procedure is as follows:- (i). Snake is placed near the contour of Region Of Interest (ROI). (ii). During an iterative process due to various internal and external forces within the image [9], the Snake is attracted towards the target. These forces control the shape and location of the snake within the image. (iii). An energy function is constructed which consist of internal and external forces to measure the appropriateness of the Contour of ROI, Minimize the

energy function (integral), which represents active contour's total energy, The internal forces are responsible for smoothness while the external forces guide the contours towards the contour of ROI.

#### IV.FEATURE EXTRACTION

Transforming the input data into the set of features is called Feature Extraction.

Geometric Features -Area, Perimeter, Circularity ,Eccentricity.

Statistical Features-Mean , Variance ,Entropy ,Correlation .

The methodology is based on the use of morphological operators contained in toolbox of Mathematical Morphology developed by SDC Information Systems, which operates coupled to software MATLAB. The application of routines in image processing is aimed initially to improve the visual quality of the features of interest in digital images, which will then afterwards be extracted. The image used in the morphological processing is in the region of President Prudente in São Paulo state and contains an excerpt from the Raposo Tavares highway-SP-280. This image was obtained from the sensor on board the satellite QUICKBIRD, which has spatial resolution of 0.61 meters. This image was chosen because it contains features of interest in the area of cartography, such as roads. Figure : illustrates the original image.

From the Figure 3 image initiated the procedure of pre-processing to facilitate the extraction of the feature. This aimed to increase the contrast of the feature of interest and reduce the prominence of noise, the operator *openrecw* was applied in the image together with the structuring element *sebox*, this is designed to create a new image through the infer-reconstruction of the original image. Operator *addm* followed with a threshold value 130, this operator creates a new image showing the difference in pixel value in the image of the runway in relation to the neighborhood "pixel wise." Increasingly seeking to get improvement in quality of the extracted feature, the image was binarized through the *binary* operator with threshold 230. The operator turned all the pixels under 230 to the value "0" (black) and those who were even higher, at "1" (white). The choice of threshold was based in analysis of the histogram of the image. Figure 4 represents the result of the application of this operator.

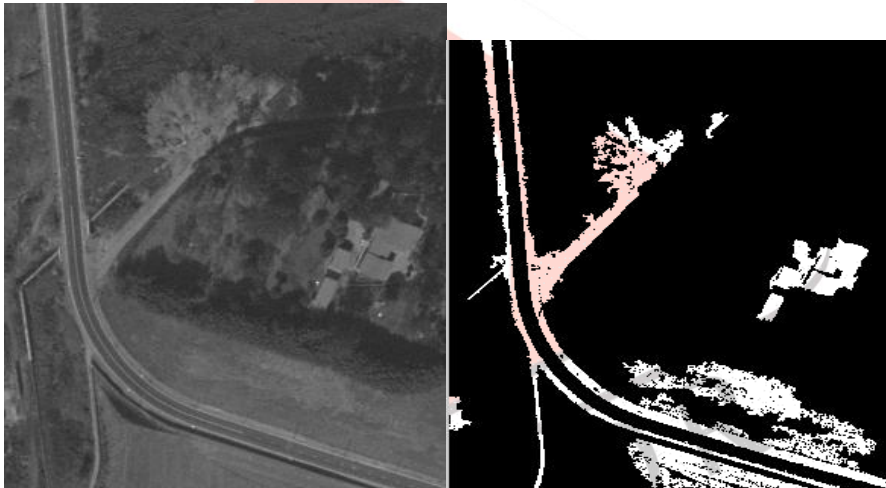


Fig.2 Binarized Image

Figure 2 shows the image with only two shades of gray (black or white) and is now possible to implement other operators with the aim to eliminate the noise surrounding the feature of interest. The operator *areaclose* (threshold 5000) was applied to remove the maximum quantity of noise possible. The result of this application is illustrated in Figure .3



Fig 3: Noise elimination

Subtracting Figure 2 and 3 resulted in Figure 4 shown below.

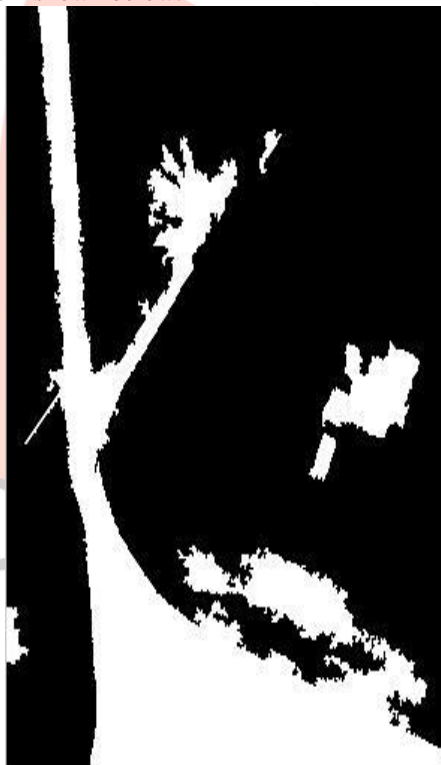


Fig 4

For the analysis of Figure 4 shows that there was a huge improvement in the extraction feature of interest, even though noises are still visual in the bottom of the image. To minimize these noises the operator *areaopen* with threshold value 4600 was applied. It also applied the operator *subm* again, subtracting the image of the previous image. Finally the operator *areaopen* was applied with a threshold 2000 enabling the removal of the last remaining noises, Figure 5 illustrates the final image of the feature extracted.

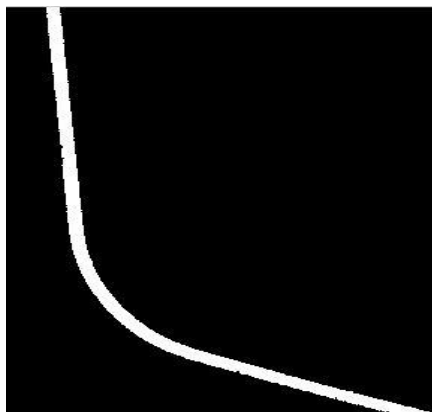


Fig.5 Detected Image

The result obtained in Figure 5 was overlaid the original image and can be seen in Figure 6.



The analysis of the results obtained in Figure 6 concluded that the process of morphological extracting was conducted in a satisfactory manner. The observation made was that there was no displacement of the feature regarding its position on the original image. This result showed that the features extracted through Mathematical Morphology may be used in procedures to update mapping.

**V. RESULTS AND ANALYSIS**

The MRI classification set consisting of 325 liver images was used on computing first-order statistics. Image blocks of 5 x 5 pixel area from the known liver regions were selected and applied with FOS texture analysis. The size of the region was determined to be 5 x 5 pixels after careful experimentation to evaluate the optimal size. The two parameters each for liver cyst, fatty liver and healthy liver features extracted from the FOS which used in the training and testing experiments were entropy and correlation for MRI. The distribution of the two data sets is shown in Table 1. A total of 325 liver images were obtained from the collaborating hospital. These MRI images consisting of 136 liver cyst samples, 91 fatty liver samples and 98 healthy liver samples.

Table 1: Number Of Samples Of Mri Images Used In The testing Sets.

<i>MRI images</i>	<i>Testing Set</i>
Liver Cyst	136
Fatty Liver	91
Healthy Liver	98
<b>Total</b>	<b>325</b>

From the analysis of the FOS results obtained, entropy and correlation are selected for classification of liver cyst, fatty liver and healthy liver for the MRI modality, due to its proven high performance as a classifier [20]. The criteria from SGLCM for liver cyst are: entropy in the range of 5.174-7.911, and correlation in the range of 5.962-6.997. As for fatty liver, entropy is in the range of 2.871-3.862 and correlation in the range of 2.300-4.932.

Finally for healthy liver classification, entropy is in the range of 0.054-1.954 and correlation within the range of 0.071-1.500.

**Table 2: Classification Of Liver Cyst, Fatty Liver And healthy Liver Using Entropy And Correlation For Mri modality.**

	Entropy		Correlation	
	Min	Max	Min	Max
Liver cyst	5.174	7.911	5.962	6.997



Fatty liver	2.871	3.862	2.300	4.932
Healthy Liver	0.054	1.954	0.071	1.500

For the FOS experiments and analysis, the parameters used for the FOS features are entropy and correlation. FOS describes the grey-level distribution without considering spatial independence. As a result, FOS can describe echogenicity of texture and the diffused variation characteristics within the ROI. The results parameters obtained from FOS for MRI liver images, are shown in Table 3 and Table 4.

Table 3: Classification Of Liver Cyst, Fatty Liver And healthy Liver Using Entropy And Correlation For Mrimodality.

Liver classes	Testing Images (T1-T28)				Entropy	
	T1-T7	T8-T14	T15-T21	T22-T28	Min	Max
Liver Cyst	5.802	5.724	6.425	6.484	5.802	6.484
	5.487	5.524	5.925	6.183	5.487	6.183
	5.477	6.554	6.072	7.854	5.477	7.854
	5.339	6.774	6.241	7.692	5.339	7.692
	5.174	6.694	6.131	7.911	<b>5.174</b>	<b>7.911</b>
	5.477	5.884	6.082	7.054	5.477	7.054
	5.884	6.145	6.281	7.692	5.884	7.692
Fatty Liver	2.880	2.869	3.101	3.248	2.880	3.248
	2.921	2.993	2.991	3.025	2.921	3.025
	2.971	3.325	3.448	3.448	2.971	3.448
	2.871	3.692	3.600	3.871	<b>2.871</b>	3.871
	2.883	2.960	3.421	3.721	2.883	3.721
	2.931	3.118	3.532	3.862	2.931	<b>3.862</b>
	3.124	3.145	3.381	3.381	3.124	3.381
Healthy Liver	0.054	0.692	1.054	1.692	<b>0.054</b>	1.692
	0.082	0.281	1.082	1.954	0.082	<b>1.954</b>
	0.554	0.784	1.054	1.281	0.554	1.281
	0.887	0.231	1.607	1.784	0.887	1.784
	0.574	0.884	1.177	1.231	0.574	1.231
	0.114	0.145	1.484	1.884	0.114	1.884
	0.774	0.954	1.074	1.145	0.774	1.145

Table 4: Classification Of Liver Cyst, Fatty Liver And Healthy Liver Using Correlation For Mri Modility

Liver classes	Testing Images (T1-T28)			Correlation	
	T8- T1-T7	T15- T14 T21	T22- T28	Min	Max
Liver Cyst	5.962	6.403	6.825	6.85 4	<b>5.962</b> 6.854
	6.127	6.241	6.325	6.48 3	6.12 7 6.483
	6.493	6.554	6.610	6.85 4	6.49 3 6.854
	6.384	6.774	6.941	6.99 7	6.38 4 <b>6.997</b>
	6.128	6.694	6.910	6.11 1	6.12 8 6.910
	6.773	6.884	6.904	6.34 1	6.77 3 6.904
	6.237	6.345	6.431	6.56 2	6.23 7 6.562
Fatty Liver	2.302	2.924	3.164	4.26 9	2.30 2 4.269
	2.300	2.811	3.119	4.70 2	<b>2.300</b> 4.702
	2.321	2.703	2.321	4.16 4	2.32 1 4.164
	2.370	2.718	3.860	4.71 8	2.37 0 4.718
	2.410	2.843	2.994	4.93 2	2.41 0 <b>4.932</b>
	3.156	3.481	3.494	4.15 6	3.15 6 4.156
	2.686	2.916	3.994	4.32 1	2.68 6 4.321
Healthy Liver	0.110	0.241	1.314	1.50 0	0.11 0 <b>1.500</b>
	0.120	0.231	1.312	1.43 1	0.12 0 1.431
	0.152	0.214	1.224	1.32 2	0.15 2 1.322
	0.133	0.231	1.167	1.31 1	0.13 3 1.311
	0.142	0.284	1.437	1.41 0	0.14 2 1.410
	0.071	0.145	1.224	1.37 4	<b>0.071</b> 1 1.374
	0.140	0.254	1.284	1.35 0	0.14 0 1.350

The results of 28 MRI liver images from the experiments are illustrated in Fig. 6 and Fig. 7. The entropy result for liver cyst, fatty liver and healthy liver for MRI range from 5.741-7.911, 2.871-3.862 and 0.054-1.954 respectively. As observed in Fig. 7, plotting the correlation of each liver tissue results in 3 curves that are distinguishable. From the preliminary study, the entropy and correlation are found to be suitable for classification of three liver classes.

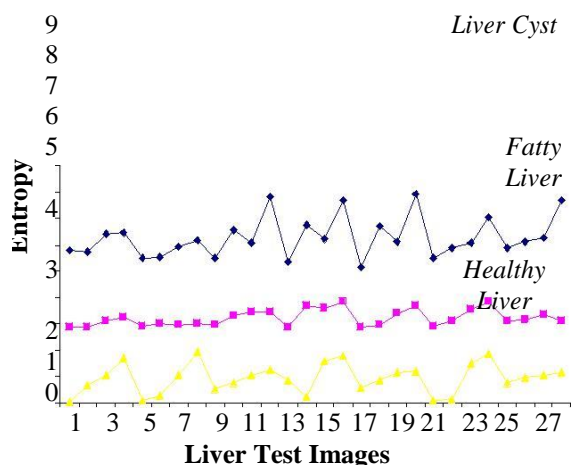


Fig. 6. Classification range for liver cyst, fatty liver and healthy liver classification using entropy.

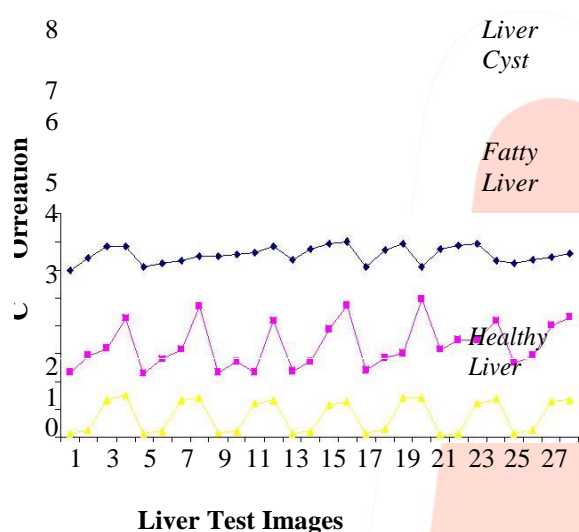


Fig. 7. Classification range for liver cyst, fatty liver and healthy liver classification using correlation.

## VI. CONCLUSION AND FUTURE WORK

In the approach described above, the analysis of FOS texture analysis has been presented, aiming to discriminate three different liver classes, namely, liver cyst, fatty liver and healthy liver from MRI liver images. The study has shown promising results and is viable in grid computing environment for classification using Globus in the use of texture analysis for the extraction of diagnostic information from images of the liver and achieved obvious liver diseases classification range using FOS in the experiments.

The inaccuracy in the results was due to images where the cysts appeared along (i.e. too flat) and not “bubble-like”. These were mistaken for the normal structures in healthy liver and not flagged by the NN classifier as cysts. As for fatty liver diagnosis, the inaccuracy was due to the features derived from FOS MRI images, intensities of the image blocks selected may contain non-liver tissues. The drawback of the classification method is the requirement of varying parameter settings for different liver classes. In order to apply this method extensively in clinical usage, standardization of the parameters is strongly recommended.

Further tests are required in order to work out the FOS’s parameters optimization procedure ensuring maximization of classification rate for a given class of liver images. Major research directions that will be investigated in the future include further improvement of FOS statistical and second-order statistical measurements for classification with grid technology, optimization of statistical parameters and implementation of the complete algorithm on a grid platform.

In particular, this paper provides results of successful preliminary diagnosis of cyst and fatty liver in the liver tissue.

## ACKNOWLEDGMENT

The authors would like to thank Dr. Logeswaran from Multimedia University and Dr. Zaharah Musa from Diagnostics Imaging Department of Hospital Selayang, for their contributions in the early phases of this project. We would like to thank reviewers for their very thoughtful comments, which improve the quality and the presentation of this paper.

## REFERENCES

- [1] L. A. Adams, J. F. Lymp, J. St Sauver and S. O. Sanderson, "The natural history of nonalcoholic fatty liver disease: a population-based cohort study," *Gastroenterology*, vol. 129, pp. 113–121, 2005. 923-926.S. Kitaguchi, S. Westland and M. R. Luo, "Suitability of Texture Analysis Methods for Perceptual Texture," in *Proceedings, 10thCongress of the International Colour Association*, 2005, vol. 10,923-926.
- [2] N. D. Cahill, C. M. Williams, S. Chen, L. A. Ray and M. M. Goodgame, "Incorporating Spatial Information into Entropy Estimates to Improve Multimodal Image Registration," in *2006<sup>3</sup>rd IEEE International Symposium on Biomedical Imaging*, pp.832-835.
- [3] K. Bommanna Raja, M. Madheswaran and K. Thyagarajah, "Evaluation of Tissue Characteristics of Kidney for Diagnosis and Classification Using First Order Statistics and RTS Invariants," presented at the 2007 ICSCN '07 International Conference on Signal Processing, Communications and Networking, 22-24 Feb. 2007, pp. 483-487. .
- [4] G. D. Kendall and T. J. Hall, "Performing fundamental image processing operations using quantized neural networks," presented at the 2002 International Conference on Image Processing and its Applications. vol. 4(1), pp. 226-229.
- [5] M. Bao, L. Guan X. Li, J. Tian and J. Yang, "Feature Extraction Using Histogram Entropies of Euclidean Distances for Vehicle Classification," presented at 2006 International Conference on Computational Intelligence and Security, vol. 1, pp. 668-673.
- [6] C. L. Gilchrist, J. Q. Xia, L. A. Setton and E. W. Hsu, "High-resolution Determination of Soft Tissue Deformations Using MRI and First-order Texture Correlation," *IEEE Transaction onMedical Imaging*, vol. 23(5), pp. 546-553, May 2004.
- [7] I. Valanis, S. G. Mougiakakou, K. S. Nikita and A. Nikita, "Computer-aided Diagnosis of CT Liver Lesions by an Ensemble of Neural Network and Statistical Classifiers," in *Proceedings ofIEEE International Joint Conference on Neural Networks*, 2004,vol. 3, pp. 1929-1934.
- [8] J. Caviedes and S. Gurbuz, "No-reference sharpness metric based on Local Edge Kurtosis," in *Proceedings International Conference on Image Processing*, 2004, vol. 3, pp. 53-56.
- [9] S. G. Mougiakakou, I. Valanis, K. S. Nikita, A. Nikita and D. Kelekis, "Characterization of CT Liver Lesions Based on Texture Features and a Multiple Neural Network Classification Scheme," in *Proceedings of the 25th Annual International Conference of the IEEE EMBS*, 2001, vol. 2(3), pp. 17-21.
- [10] S. W. Chee, K. Pyun and R. M. Gray, "Automatic Object Segmentation in Images with Low Depth of Field," presented at *International Conference on Image Processing*, June 2002, vol. 3, 805-808.
- [11] H. Jiang and H. Fujita, "Research on Segmentation Method of Multi-Region Liver Image," *WCICA 2006 The Sixth WorldCongress on Intelligent Control and Automation*, June 2006, vol.2, pp. 9992-9995.
- [12] C. P. Loizou, C. S. Pattichis, C. I. Christodoulou, R. S. H. Istepanian, M. Pantziaris and A. Nicolaidis, "Comparative Evaluation of Deskpeckle Filtering in Ultrasound Imaging of the Carotid Artery," *IEEE Transactions on Ultrasonics,Ferroelectrics and Frequency Control*, Oct 2005, vol. 52(10), pp.1653-1669.
- [13] M. Gletsos, S. G. Mougiakakou, G. K. Matsopoulos, K. S. Nikita, A. S. Nikita and D. Kelekis, "A Computer-aided Diagnostic System to Characterize CT Focal Liver Lesions: Design and Optimization of a Neural Network Classifier," *IEEE Transactionson Information Technology in Biomedicine*, 2003, vol. 7(3), pp.153-162.
- [14] K. Bommanna Raja, M. Madheswaran and K. Thyagarajah, "Evaluation of Tissue Characteristics of Kidney for Diagnosis and Classification Using First Order Statistics and RTS Invariants," presented at the 2007 ICSCN '07 International Conference on Signal Processing, Communications and Networking, 22-24 Feb. 2007, pp. 483-487. .
- [15] G. D. Kendall and T. J. Hall, "Performing fundamental image processing operations using quantized neural networks," presented at the 2002 International Conference on Image Processing and its Applications. vol. 4(1), pp. 226-229.
- [16] M. Bao, L. Guan X. Li, J. Tian and J. Yang, "Feature Extraction Using Histogram Entropies of Euclidean Distances for Vehicle Classification," presented at 2006 International Conference on Computational Intelligence and Security, vol. 1, pp. 668-673.
- [17] C. L. Gilchrist, J. Q. Xia, L. A. Setton and E. W. Hsu, "High-resolution Determination of Soft Tissue Deformations Using MRI and First-order Texture Correlation," *IEEE Transaction onMedical Imaging*, vol. 23(5), pp. 546-553, May 2004.
- [18] I. Valanis, S. G. Mougiakakou, K. S. Nikita and A. Nikita, "Computer-aided Diagnosis of CT Liver Lesions by an Ensemble of Neural Network and Statistical Classifiers," in *Proceedings ofIEEE International Joint Conference on Neural Networks*, 2004,vol. 3, pp. 1929-1934.
- [19] J. Caviedes and S. Gurbuz, "No-reference sharpness metric based on Local Edge Kurtosis," in *Proceedings InternationalConference on Image Processing*, 2004, vol. 3, pp. 53-56.
- [20] S. G. Mougiakakou, I. Valanis, K. S. Nikita, A. Nikita and D. Kelekis, "Characterization of CT Liver Lesions Based on Texture Features and a Multiple Neural Network Classification Scheme," in *Proceedings of the 25th Annual International Conference of the IEEE EMBS*, 2001, vol. 2(3), pp. 17-21.
- [21] S. W. Chee, K. Pyun and R. M. Gray, "Automatic Object Segmentation in Images with Low Depth of Field," presented at *International Conference on Image Processing*, June 2002, vol. 3, 805-808.
- [22] H. Jiang and H. Fujita, "Research on Segmentation Method of Multi-Region Liver Image," *WCICA 2006 The Sixth WorldCongress on Intelligent Control and Automation*, June 2006, vol.2, pp. 9992-9995.
- [23] C. P. Loizou, C. S. Pattichis, C. I. Christodoulou, R. S. H. Istepanian, M. Pantziaris and A. Nicolaidis, "Comparative Evaluation of Deskpeckle Filtering in Ultrasound Imaging of the Carotid Artery," *IEEE Transactions on Ultrasonics,Ferroelectrics and Frequency Control*, Oct 2005, vol. 52(10), pp.1653-1669.

- [24] M. Gletsos, S. G. Mougiakakou, G. K. Matsopoulos, K. S. Nikita, A. S. Nikita and D. Kelekis, "A Computer-aided Diagnostic System to Characterize CT Focal Liver Lesions: Design and Optimization of a Neural Network Classifier," IEEE Transactions on Information Technology in Biomedicine, 2003, vol. 7(3), pp.153-162.

